

Renewable Dehydrogenase-Based Interfaces for Bioelectronic Applications

Brian L. Hassler,[†] Neeraj Kohli,[†] J. Gregory Zeikus,[‡] Ilsoon Lee,[†] and Robert M. Worden^{*†}

Departments of Chemical Engineering and Materials Science and of Biochemistry and Molecular Biology, Michigan State University, East Lansing, Michigan 48824

Received February 14, 2007. In Final Form: April 11, 2007

Bioelectronic interfaces that establish electrical communication between redox enzymes and electrodes have potential applications as biosensors, biocatalytic reactors, and biological fuel cells. However, these interfaces contain labile components, including enzymes and cofactors, which have limited lifetimes and must be replaced periodically to allow long-term operation. Current methods to fabricate bioelectronic interfaces do not allow facile replacement of these components, thus limiting the useful lifetime of the interfaces. In this paper we describe a versatile new fabrication approach that binds the enzymes and cofactors using reversible ionic interactions. This approach allows the interface to be removed via a simple pH change and then replaced to fully regenerate the biocatalytic activity. The positively charged polyelectrolyte poly(ethylenimine) was used to ionically bond a dehydrogenase enzyme and its cofactor to a gold electrode that was functionalized with 3-mercaptopropionic acid and the electron mediator toluidine blue O. By reducing the pH, the surface-bound 3-mercaptopropionic acid was protonated, disrupting the ionic bonds and releasing the enzyme-modified polyelectrolyte. After neutralization, fresh enzyme and cofactor were bound, regenerating the bioelectronic interface. Cyclic voltammetry, chronoamperometry, constant potential amperometry, electrochemical impedance spectroscopy, and Fourier transform infrared spectroscopy analyses were used to characterize the bioelectronic interfaces. For the two enzymes tested (secondary alcohol dehydrogenase and sorbitol dehydrogenase) and their respective cofactors (β -nicotinamide adenine dinucleotide phosphate and β -nicotinamide adenine dinucleotide), the reconstituted interface exhibited a surface coverage, an electron-transfer coefficient, and a turnover rate similar to those of the original interface.

Introduction

Bioelectronic interfaces achieve electrical communication between redox enzymes and an electrode.^{1–5} Development of a bioelectronic interface is especially challenging for cofactor-dependent dehydrogenase enzymes, whose activity requires the presence of an electron-carrying cofactor (e.g., β -nicotinamide adenine dinucleotide (NAD⁺)) in the Rossmann fold of the protein. The cofactor transmits electrons between the electron source or sink (e.g., an electrode) and the redox center of the protein. Direct electron transfer between the cofactor and a gold electrode is not kinetically favored, requiring the use of high overpotentials^{6,7} which may lead to cofactor degradation and interference by compounds such as ascorbic acid and molecular oxygen.^{3,8} These problems can be circumvented by using an electron mediator to shuttle electrons between the electrode and cofactor at moderate potentials.^{9,10} Several approaches have been

used to achieve mediated electron exchange, including immobilization of the enzymes in conductive polymers^{5,11} and construction of a redox relay that conducts electrons between the enzyme and electrode.^{12,13}

To achieve efficient electron transfer, Willner and co-workers assembled a linear molecular chain consisting of the electrode, mediator, cofactor, and enzyme.^{14,15} This arrangement allowed unimpeded access of the cofactor to its binding site on the enzyme, provided efficient, multistep electron transfer, and prevented component loss due to diffusion. However, this approach uses the bifunctional mediator pyrroloquinoline quinone (PQQ), whose high cost (about \$30000 per gram) makes it prohibitively expensive for many commercial applications. To overcome this problem, we developed an interface suitable for inexpensive, monofunctional electron mediators, such as toluidine blue O (TBO), neutral red, and Nile blue A.^{16,17}

Dehydrogenase enzymes and their cofactors have limited useful lifetimes, due to natural degradation processes.^{18–20} The above-mentioned interface fabrication methods involve

* To whom correspondence should be addressed. E-mail: worden@egr.msu.edu.

[†] Department of Chemical Engineering and Materials Science.

[‡] Department of Biochemistry and Molecular Biology.

(1) Armstrong, F. A.; Heering, H. A.; Hirst, J. *Chem. Soc. Rev.* **1997**, *26* (3), 169–179.

(2) Armstrong, F. A.; Wilson, G. S. *Electrochim. Acta* **2000**, *45* (15–16), 2623–2645.

(3) Park, D. H.; Laivenieks, M.; Guettler, M. V.; Jain, M. K.; Zeikus, J. G. *Appl. Environ. Microbiol.* **1999**, *65* (7), 2912–2917.

(4) Park, D. H.; Zeikus, J. G. *J. Bacteriol.* **1999**, *181* (8), 2403–2410.

(5) Chen, T.; Barton, S. C.; Binyamin, G.; Gao, Z. Q.; Zhang, Y. C.; Kim, H. H.; Heller, A. *J. Am. Chem. Soc.* **2001**, *123* (35), 8630–8631.

(6) Blaedel, W. J.; Jenkins, R. A. *Anal. Chem.* **1975**, *47* (8), 1337–1343.

(7) Schmamel, C. O.; Santhanam, K. S. V.; Elving, P. J. *J. Am. Chem. Soc.* **1975**, *97* (18), 5083–5092.

(8) Ramesh, P.; Sivakumar, P.; Sampath, S. *Electroanalysis* **2003**, *15* (23–24), 1850–1858.

(9) Ozdemir, A.; Tuncel, A. *J. Appl. Polym. Sci.* **2000**, *78* (2), 268–277.

(10) Senel, S.; Camli, S. T.; Tuncel, M.; Tuncel, A. *J. Chromatogr., B: Anal. Technol. Biomed. Life Sci.* **2002**, *769* (2), 283–295.

(11) Emr, S. A.; Yacynych, A. M. *Electroanalysis* **1995**, *7* (10), 913–923.

(12) Degani, Y.; Heller, A. *J. Phys. Chem.* **1987**, *91* (6), 1285–1289.

(13) Zimmermann, H.; Lindgren, A.; Schuhmann, W.; Gorton, L. *Chem.—Eur. J.* **2000**, *6* (4), 592–599.

(14) Zayats, M.; Katz, E.; Willner, I. *J. Am. Chem. Soc.* **2002**, *124* (49), 14724–14735.

(15) Willner, B.; Katz, E.; Willner, I. *Curr. Opin. Biotechnol.* **2006**, *17* (6), 589–596.

(16) Hassler, B. L.; Dennis, M.; Laivenieks, M.; Zeikus, J. G.; Worden, R. M. Submitted for publication.

(17) Hassler, B. L.; Worden, R. M. *Biosens. Bioelectron.* **2006**, *21* (11), 2146–2154.

(18) Burdette, D. S.; Tchernajenko, V.; Zeikus, J. G. *Enzyme Microb. Technol.* **2000**, *27* (1–2), 11–18.

(19) De Temino, D. M.; Hartmeier, W.; Ansorge-Schumacher, M. B. *Enzyme Microb. Technol.* **2005**, *36* (1), 3–9.

(20) Wang, S. Y.; Feng, Y.; Zhang, Z. M.; Zheng, B. S.; Li, N.; Cao, S. G.; Matsui, I.; Kosugi, Y. *Arch. Biochem. Biophys.* **2003**, *411* (1), 56–62.

covalent linkages and make no provision for removal and replacement of degraded components. For long-term operation, new interface-assembly methods must be developed that allow facile removal and replacement of the cofactor and enzyme.

Layer-by-layer (LbL) deposition provides a mechanism by which target molecules can be reversibly bound to an interface and later released.^{21,22} In this method, electrostatic attractions allow alternating layers of oppositely charged polyelectrolytes to be sequentially adsorbed onto virtually any surface.^{23–25} The resulting polyelectrolyte multilayers (PEMs) provide effective and economical organic thin films that have been extended to organic dyes,^{26,27} colloids,²⁸ cells,^{29,30} and biomaterials.^{31,32} Proteins, including catalase,^{33–35} glucose oxidase,^{33,36,37} and polyphenol oxidase^{38,39} have been incorporated into LbL films. However, dehydrogenase enzymes and their cofactors have yet to be incorporated.

In this paper we present a novel method based on LbL self-assembly to fabricate a renewable bioelectronic interface in which the enzyme and cofactor can be removed and replaced. The polycation poly(ethylenimine) (PEI) was used to couple the electron mediator, cofactor, and enzyme to a carboxylic acid-modified gold electrode in such a way that mediated electron transfer was achieved. Decreasing the pH of the solution protonated the surface-bound carboxylic acid groups, disrupting the ionic bonds and releasing the enzyme and cofactor. After neutralization, fresh enzyme and cofactor could be bound, allowing the interface to be reconstituted. Cyclic voltammetry, Fourier transform infrared spectroscopy (FTIR), constant-potential amperometry, and chronoamperometry were used to characterize the interface and to show that the original and reconstituted interfaces exhibited similar electrochemical properties. To demonstrate the versatility of the approach, results are presented for two enzymes, secondary alcohol dehydrogenase (2° ADH) and sorbitol dehydrogenase (SDH), and two cofactors, NAD⁺ and β -nicotinamide adenine dinucleotide phosphate (NADP⁺).

Materials and Methods

Media and Strains. The 2° ADH from *Thermoanaerobacter ethanolicus* was produced using *Escherichia coli* (DH5 α pADH BIM1-kan) and then purified as previously described.¹⁶ Purified sorbitol dehydrogenase (SDH) from *Pseudomonas* sp. *KS-E1806* was provided by the Kikkoman Corp. (Chiba, Japan).⁴⁰

Chemicals. Tryptone, yeast extract, dithiothreitol (DTT), kanamycin, and ampicillin were purchased from Fisher Scientific (Pittsburgh, PA). All other chemicals, including 3-mercaptopropionic acid (MPA), 1-ethyl-3-(3-(dimethylamino)propyl)carbodiimide (EDC), *N*-hydroxysuccinimide (NHS), TBO, PEI, 3-carboxyphenylboronic acid (CBA), NAD⁺, NADP⁺, glutaric dialdehyde (25% in water), 2-propanol, ethanol, 2-butanol, 2-pentanol, D-sorbitol, l-sorbose, D-arabinose, and D-glucose were obtained from Sigma-Aldrich (St. Louis, MO). Ultrapure water (18.2 M Ω) was supplied by a Barnstead Nanopure-UV four-stage purifier (Barnstead International, Dubuque, IA).

Formation of the Bioelectronic Interface. Gold electrodes (1 cm \times 1.5 cm rectangular electrodes, roughness factor approximately 1.2) were cleaned by immersion in piranha solution (70% by volume concentrated sulfuric acid and 30% by volume 30% aqueous hydrogen peroxide) for 30 s. The electrodes were treated with a Harrick plasma cleaner (Harrick Scientific Corp., Brooding Ossining, NY) for 1 min under a 50 sccm flow of oxygen at a pressure of 0.15 Torr. The electrodes were then rinsed with deionized (DI) water for 10 min.

The cleaned gold electrodes were soaked in a 0.1 M MPA solution in ethanol for 1 h at room temperature (25 \pm 2 °C) and thoroughly rinsed with ethanol and DI water to remove weakly adsorbed MPA. The MPA-modified gold electrodes were incubated for 2 h in 100 μ M TBO in a 0.1 M phosphate buffer solution (PBS), pH 7.4, in the presence of 2 mM NHS and 2 mM EDC, resulting in the formation of an amide linkage between the TBO and the MPA (MPA–TBO). The MPA–TBO-modified electrodes were soaked in a 10 mM aqueous solution of PEI solution containing 0.1 M NaCl, pH 7.0, forming an MPA–TBO–PEI-modified interface. We propose the PEI adsorbs to the MPA–TBO-modified electrode through electrostatic interactions between the unreacted MPA and hydrophobic interactions with the TBO-modified interface. A 5 mM aqueous solution of CBA solution was activated at room temperature in the presence of 2 mM NHS and 2 mM EDC in PBS for 2 h. The NHS-modified CBA was then reacted with the MPA–TBO–PEI-functionalized electrodes for 1 h at room temperature, resulting in an amide linkage between the CBA and the amine group of the PEI. The resulting MPA–TBO–PEI–CBA-modified electrodes were reacted with a 1 mM solution of either NAD⁺ or NADP⁺ in PBS, pH 7.4, for 1 h and then washed with water. Scheme 1 illustrates the steps involved in functionalizing the electrode with MPA, TBO, PEI, and the respective cofactor (NAD⁺ or NADP⁺). To bind 2° ADH, the MPA–TBO–PEI–NADP⁺-functionalized gold electrodes were reacted with a 4.4 mg mL⁻¹ solution of 2° ADH in 0.1 M PBS, pH 7.4, for 1 h at room temperature and cross-linked with 25% (v/v) glutaric acid in water for 20 min. To bind SDH, the MPA–TBO–PEI–NAD⁺-functionalized electrodes were incubated with 2.3 mg mL⁻¹ SDH in 0.1 M PBS, pH 7.4, for 1 h at room temperature and cross-linked with 25% (v/v) glutaric acid in water for 20 min. The resulting 2° ADH and SDH-modified interfaces were used for the biocatalytic oxidation of 2-propanol and d-sorbitol, respectively.

The cofactor- and enzyme-functionalized PEI layer was removed by incubating the electrode in 0.01 M HCl (pH 2.0) for 30 min. For values below the pK_a of MPA (pK_a \approx 4.3), the carboxylic acid group is protonated, thus decreasing the electrostatic interaction between the surface-bound MPA and the 2° ADH-modified PEI and allowing the PEI to disengage from the surface. To reassemble the interface, PEI, CBA, NADP⁺, and 2° ADH were reattached onto the TBO-modified MPA monolayer using the protocol described above.

(21) Yun, D. H.; Song, M. J.; Hong, S. I.; Kang, M. S.; Min, N. K. *J. Korean Phys. Soc.* **2005**, *47*, S445–S449.

(22) Wu, Z. Y.; Guan, L. R.; Shen, G. L.; Yu, R. Q. *Analyst* **2002**, *127* (3), 391–395.

(23) Decher, G.; Hong, J. D. *Ber. Bunsen-Ges.* **1991**, *95* (11), 1430–1434.

(24) Decher, G.; Hong, J. D. *Makromol. Chem., Macromol. Symp.* **1991**, *46*, 321–327.

(25) Decher, G.; Hong, J. D.; Schmitt, J. *Thin Solid Films* **1992**, *210* (1–2), 831–835.

(26) Masadome, T.; Imato, T. *Talanta* **2003**, *60* (4), 663–668.

(27) Qian, J. M.; Suo, A. L.; Yao, Y.; Jin, Z. H. *Clin. Biochem.* **2004**, *37* (2), 155–161.

(28) Lvov, Y.; Caruso, F. *Anal. Chem.* **2001**, *73* (17), 4212–4217.

(29) Kidambi, S.; Lee, I.; Chan, C. *J. Am. Chem. Soc.* **2004**, *126* (50), 16286–16287.

(30) Berg, M. C.; Yang, S. Y.; Hammond, P. T.; Rubner, M. F. *Langmuir* **2004**, *20* (4), 1362–1368.

(31) Ai, H.; Fang, M.; Jones, S. A.; Lvov, Y. M. *Biomacromolecules* **2002**, *3* (3), 560–564.

(32) Ai, H.; Ihlemann, J.; Hellsten, Y.; Lauritzen, H.; Hardie, D. G.; Galbo, H.; Ploug, T. *Am. J. Physiol. Endocrinol. Metab.* **2002**, *282* (6), E1291–E1300.

(33) Shutava, T. G.; Kommireddy, D. S.; Lvov, Y. M. *J. Am. Chem. Soc.* **2006**, *128* (30), 9926–9934.

(34) Wang, Y. J.; Caruso, F. *Chem. Mater.* **2005**, *17* (5), 953–961.

(35) Shi, L. X.; Lu, Y. X.; Sun, J.; Zhang, J.; Sun, C. Q.; Liu, J. Q.; Shen, J. C. *Biomacromolecules* **2003**, *4* (5), 1161–1167.

(36) Antipov, A. A.; Sukhorukov, G. B. *Adv. Colloid Interface Sci.* **2004**, *111* (1–2), 49–61.

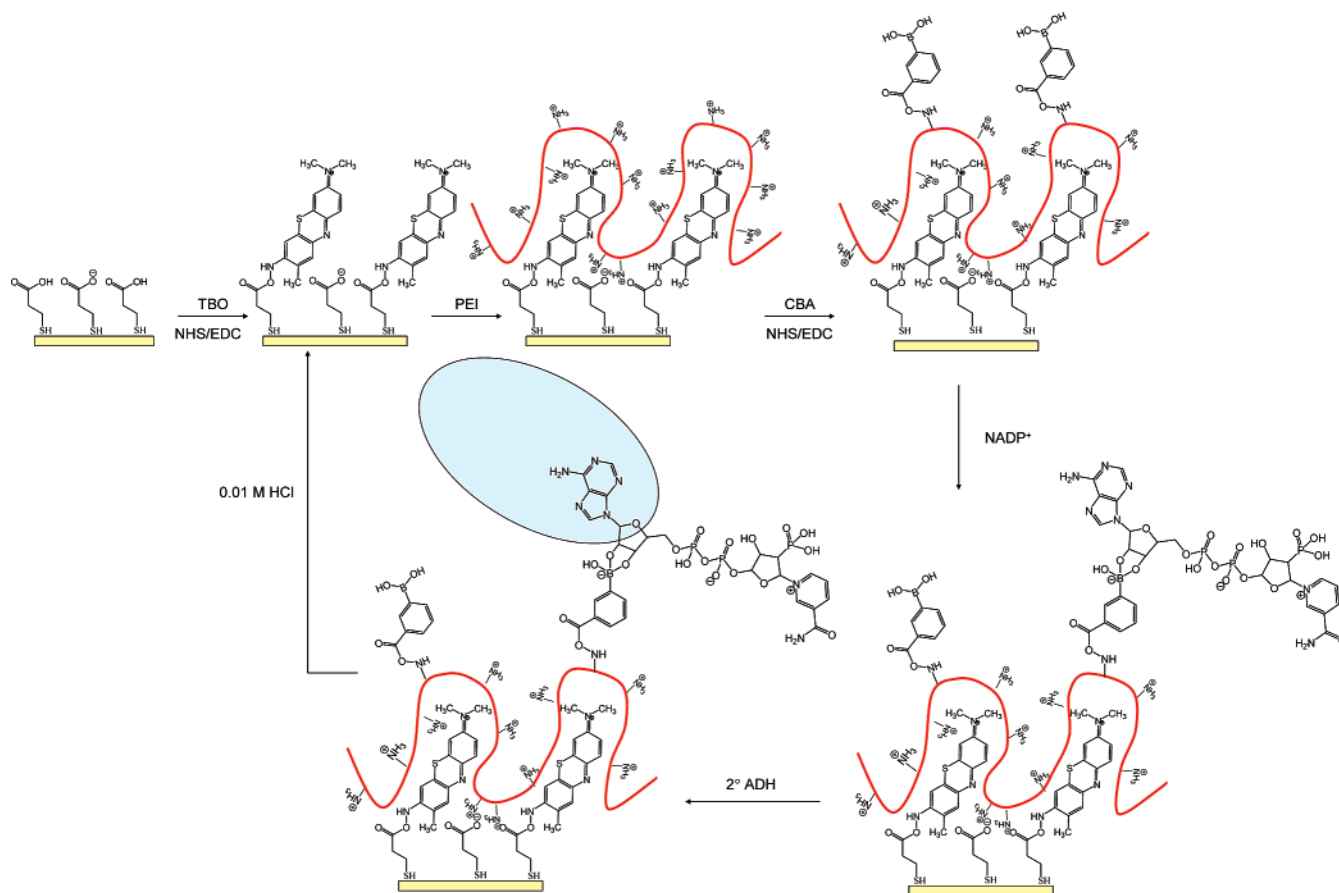
(37) Zhao, W.; Xu, J. J.; Shi, C. G.; Chen, H. Y. *Langmuir* **2005**, *21* (21), 9630–9634.

(38) Coche-Guerente, L.; Desbrieres, J.; Fatissou, J.; Labbe, P.; Rodriguez, M. C.; Rivas, G. *Electrochim. Acta* **2005**, *50* (14), 2865–2877.

(39) Forzani, E. S.; Teijelo, M. L.; Nart, F.; Calvo, E. J.; Solis, V. M. *Biomacromolecules* **2003**, *4* (4), 869–879.

(40) Minamihara, T.; Suzuki, M. *J. Ferment. Bioeng.* **1997**, *84* (3), 254–256.

Scheme 1. Sequential Steps in the Formation of an Integrated MPA–TBO–PEI–NADP⁺–2° ADH-Functionalized Gold Electrode



Electrochemical Measurements. A conventional three-electrode cell consisting of the enzyme-modified gold working electrode, a platinum auxiliary electrode, and a silver/silver chloride (Ag/AgCl) reference electrode was used for electrochemical measurement. Cyclic voltammetry, chronoamperometry, and constant-potential amperometry were performed in a grounded Faraday cage using an electrochemical analyzer (CHI660 B, CH Instruments, Austin, TX) connected to a personal computer. Chronoamperometric experiments were conducted by stepping the potential of the working electrode from -200 to 400 mV, triggering oxidation of 2-propanol or D-sorbitol in the vicinity of the electrode. Origin (version 7.6, OriginLab, Northampton, MA) was used to fit kinetic models to the resulting current vs time data. Constant-potential amperometry experiments were conducted by holding the potential constant at 400 mV, which causes oxidation at the interface. Cyclic voltammetric experiments were conducted by sweeping the potential of the working electrode between -200 and $+400$ mV at a scan rate of 100 mV s⁻¹, causing analyte in the vicinity of the electrode to be oxidized in the positive direction and reduced in the reverse direction. Electrochemical measurements were made in 0.1 M PBS, pH 7.4, at room temperature for 2° ADH and in 0.1 M glycine–NaOH buffer, pH 9.0, at 40 °C for SDH. All electrochemical measurements were made using an electrode with a controlled surface area of 0.16 cm².

Electrochemical impedance spectroscopy (EIS) was used to investigate the sequential assembly of mediators, cofactors, and enzymes onto the gold electrode. To ensure complete characterization of the interface, EIS measurements were made over five frequency decades, from 10^{-1} to 10^4 Hz, at an open circuit potential of 221 mV. Impedance measurements were performed using an electrochemical analyzer composed of a potentiostat/frequency response detector (CHI660 B) connected to a personal computer running Electrochemical Bench software. The data were displayed as a Nyquist plot (imaginary impedance (Z_{im}) vs real impedance (Z_{re})).

A simple Randles electrical equivalent circuit model⁴¹ was fit to data using commercial software (Zview, version 2.1b, Scribner Associates Inc., Southern Pines, NC).

Results and Discussion

Figure 1 shows the FTIR spectra for gold electrodes modified with (A) MPA, (B) MPA–TBO, and (C) MPA–TBO–PEI–NADP⁺–2° ADH. Figure 1D shows the FTIR spectrum after the MPA–TBO–PEI–NADP⁺-modified electrode was washed with 0.01 M HCl, and Figure 1E shows the fully reconstituted MPA–TBO–PEI–NADP⁺–2° ADH interface. Figure 1A shows peaks around 1710 and 1420 cm⁻¹ corresponding to the carboxylic acid (C=O) vibration and C–H bend, respectively, consistent with literature reports.^{42–44} Figure 1B shows absorption peaks at 1626 and 1450 cm⁻¹ which correspond to the amide I' (C=O) stretching and amide II' (N–H) bending,⁴⁵ suggesting the formation of an amide bond between the MPA and TBO. Figure 1C shows absorption peaks at 1680 and 1540 cm⁻¹ which correspond to the carboxylic acid (C=O) vibration and amine (N–H) bending, respectively. These peaks are consistent with enzyme adsorption.⁴⁶ The absorption peaks at 1680 and 1540

(41) Phillips, R. K. R.; Omanovic, S.; Roscoe, S. G. *Langmuir* **2001**, *17* (8), 2471–2477.

(42) Sun, L.; Kepley, L. J.; Crooks, R. M. *Langmuir* **1992**, *8* (9), 2101–2103.

(43) Ihs, A.; Liedberg, B. *J. Colloid Interface Sci.* **1991**, *144* (1), 282–292.

(44) Nuzzo, R. G.; Dubois, L. H.; Allara, D. L. *J. Am. Chem. Soc.* **1990**, *112* (2), 558–569.

(45) Meersman, F.; Wang, J.; Wu, Y. Q.; Heremans, K. *Macromolecules* **2005**, *38* (21), 8923–8928.

(46) Masuda, S.; Hasegawa, K.; Ishii, A.; Ono, T. *Biochemistry* **2004**, *43* (18), 5304–5313.

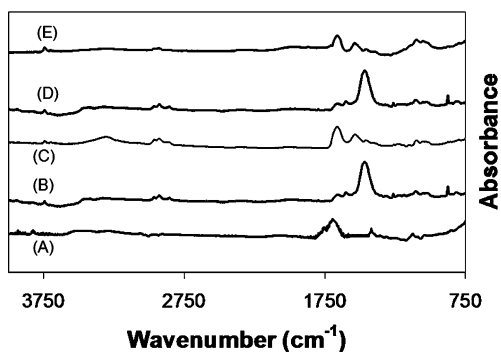


Figure 1. Average FTIR absorption spectra for the bioelectronic interface at several intermediate stages of assembly: (A) MPA, (B) MPA-TBO, (C) MPA-TBO-PEI-NAD⁺-2° ADH, (D) MPA-TBO (after removal of the 2° ADH-modified PEI), and (E) MPA-TBO-PEI-NADP⁺-2° ADH (after readsorption of the PEI and NAD⁺).

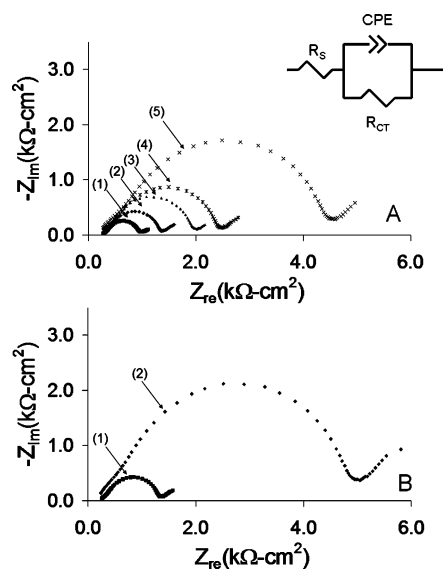


Figure 2. (A) Nyquist plots of (1) MPA-, (2) MPA-TBO-, (3) MPA-TBO-PEI-, (4) MPA-TBO-PEI-NAD⁺-, and (5) MPA-TBO-PEI-NADP⁺-2° ADH-modified electrodes in Fe(CN)₆^{3-/4-} in 0.1 M PBS, pH 7.4, recorded at 230 mV and room temperature. Inset: equivalent electrical circuit used to model the electrical impedance spectrum data. (B) Nyquist plots for the (1) MPA-TBO-PEI-NAD⁺-2° ADH-modified electrode after it was washed with 0.01 M HCl and the (2) MPA-TBO-PEI-NAD⁺-2° ADH-modified electrode after reconstitution.

cm⁻¹ of the MPA-TBO-PEI-NADP⁺-2° ADH interface disappeared after the electrode was washed with HCl (Figure 1D), while the peaks at 1626 and 1450 cm⁻¹ remained, suggesting the removal of the NADP⁺-2° ADH-modified PEI. Upon the reattachment of the NADP⁺-2° ADH-modified PEI, the absorption bands at 1680 and 1540 cm⁻¹ reappeared (Figure 1E). Collectively, these results are consistent with the assembly of the MPA-TBO-PEI-NAD⁺-2° ADH interface, removal of the NADP⁺-2° ADH-modified PEI at reduced pH, and subsequent reconstitution of the interface.

Figure 2A shows Nyquist plots for the MPA-, MPA-TBO-, MPA-TBO-PEI-, MPA-TBO-PEI-NADP⁺-, and MPA-TBO-PEI-2° ADH-modified electrodes (curves 1–5, respectively). At high frequencies Nyquist plots exhibit a semicircular domain, whose radius is proportional to the charge-transfer resistance. At low frequencies, the plot has a linear region associated with mass transport limitations. In the analysis of the EIS data, a modified Randles equivalent circuit with a solution

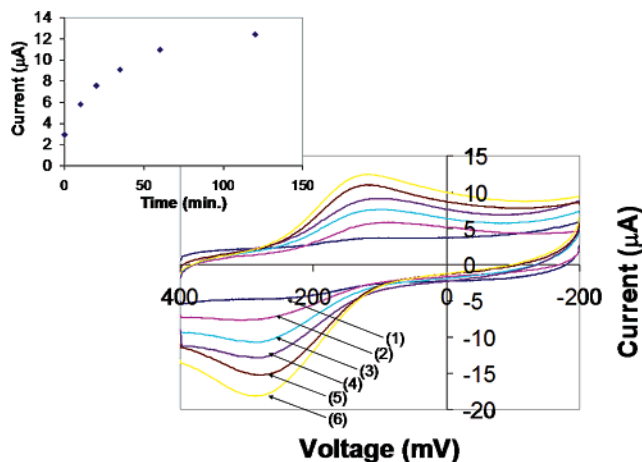


Figure 3. Cyclic voltammograms of the MPA-TBO-PEI-NADP⁺-functionalized electrode at various times of 2° ADH reconstitution: (1) 2, (2) 5, (3) 15, (4) 30, (5) 60, and (6) 120 min. The data were recorded in room-temperature PBS containing 30 mM 2-propanol at a potential scan rate of 100 mV s⁻¹. Inset: peak electrocatalytic current at various time intervals.

resistance (R_s), charge-transfer resistance (R_{CT}), and constant phase element (CPE), Figure 2A, inset, was used to analyze the impedance data, as proposed by Brug et al.⁴⁷ Fitting the equivalent-circuit model to the EIS data using Z-view software gave R_{CT} values of 0.98, 1.4, 2.0, 2.5, and 4.6 kΩ cm² for the MPA-, MPA-TBO-, MPA-TBO-PEI-, MPA-TBO-PEI-NADP⁺-, and MPA-TBO-PEI-2° ADH-modified electrodes, respectively. The increase in R_{CT} with each sequential layer is consistent with the successive deposition of additional layers, thus providing evidence of electrode formation. Figure 2B, curve 1, shows the Nyquist plot for the MPA-TBO-PEI-2° ADH-modified electrodes after they were washed with 0.01 M HCl. The value of R_{CT} (1.5 kΩ cm²) was approximately equal to that for the MPA-TBO-modified electrode, suggesting that the HCl removed the NADP⁺- and 2° ADH-modified PEI. After the procedure used to attach PEI, CBA, NADP⁺, and 2° ADH was repeated, R_{CT} (4.9 kΩ cm², curve 2) returned to the value corresponding to the MPA-TBO-PEI-2° ADH-modified electrode, providing evidence that the bioelectronic interface was reconstituted.

Figure 3 shows cyclic voltammograms for the MPA-TBO-PEI-NADP⁺-modified electrode in 25 mM 2-propanol at different times of 2° ADH adsorption. Figure 3, inset, shows the peak anodic current at various adsorption times. A first-order kinetic model was fit to the data, giving a time constant of 33 min. The time constant is similar to that obtained for 2° ADH adsorption on the cysteine (CYS)-TBO-NADP⁺-modified interface formed on a gold-coated silicon wafer (43 min).¹⁷

Figure 4A shows the chronoamperometric current response for the MPA-TBO-PEI-NADP⁺-2° ADH-modified electrode in the presence of 2-propanol following a step change in potential from -200 to +400 mV. The charge-transfer dynamics are dependent on the spatial orientation of the components composing the interface. Redox components with multiple binding modes may exhibit a rate constant for each mode.¹⁴ Because NADP⁺ has a single *cis*-diol moiety capable of forming a boronic acid linkage (Scheme 1), a single-exponential decay model,⁴⁸ eq 1,

$$I = k_{et}Q \exp(-k_{et}t) \quad (1)$$

(47) Brug, G. J.; Vandeneeden, A. L. G.; Sluytersrehabach, M.; Sluyters, J. H. *J. Electroanal. Chem.* **1984**, 176 (1–2), 275–295.

(48) Katz, E.; Willner, I. *Langmuir* **1997**, 13 (13), 3364–3373.

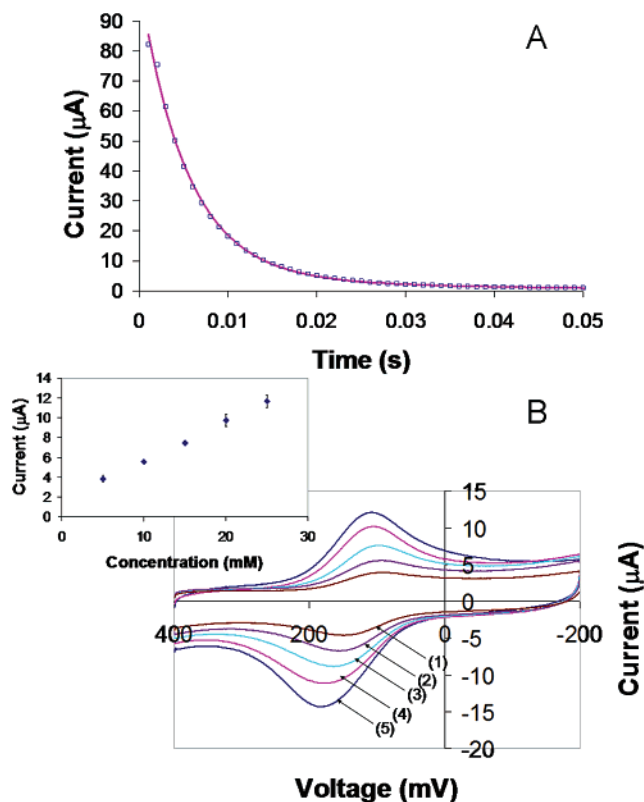


Figure 4. (A) Chronoamperometric current transient following a potential step from $E_{\text{initial}} = -200$ mV to $E_{\text{final}} = +400$ mV for the MPA-TBO-PEI-NADP⁺-2° ADH-functionalized electrode. (B) Cyclic voltammograms of the MPA-TBO-PEI-NADP⁺-2° ADH-functionalized electrode in the presence of different concentrations of 2-propanol: (1) 5, (2) 10, (3) 15, (4) 20, and (5) 25 mM. The data were recorded in room-temperature PBS at a potential scan rate of 100 mV s⁻¹. Inset: peak electrocatalytic current at various 2-propanol concentrations. The error bars indicate the mean \pm standard deviation ($n = 3$).

was fit to the data. In this equation, k_{et} is the electron-transfer rate constant and Q is the charge associated with oxidation following the change in potential. The resulting k_{et} value was 190 s⁻¹. The surface coverage (Γ) of active enzyme was calculated using eq 2,¹⁴

$$\Gamma = Q/nFA \quad (2)$$

where F is Faraday's constant, A is the electrode area, and n is the number of electrons transferred ($n = 2$) in the reaction. The resulting Γ value of 1.6×10^{-11} mol cm⁻² represents the surface density of functional bioelectronic complexes able to achieve multistep electron transfer between the enzyme and electrode. This Γ value is comparable to that measured for a CYS-TBO-NADP⁺-2° ADH-modified gold-coated silicon wafer (2.1×10^{-11} mol cm⁻²).¹⁶

Figure 4B shows the cyclic voltammograms of the reconstituted enzyme electrodes at different 2-propanol concentrations. The anodic wave began at the oxidation potential of the bound TBO (200 mV), suggesting that TBO mediates the electron transfer between the bound cofactor and the electrode. The peak anodic current varies linearly with the 2-propanol concentration, Figure 4B, inset, indicating the interface can function as a 2-propanol biosensor. The slope of this calibration curve, $2.5 \mu\text{A mM}^{-1}$ cm⁻², is a measure of the biosensor's sensitivity. At higher concentrations, the anodic current reaches a saturation value ($I_{\text{cat}}^{\text{sat}} = 12 \mu\text{A}$). This value was used to calculate a maximum

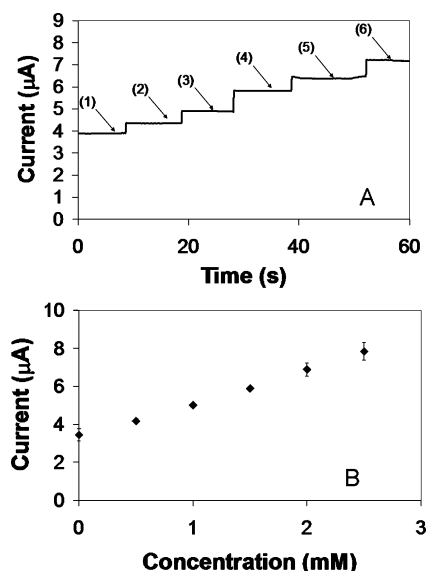


Figure 5. (A) Amperometric measurements for the MPA-TBO-PEI-NADP⁺-2° ADH-modified electrode in the presence of different concentrations of acetone at a potential of 400 mV: (1) 0, (2) 0.5, (3) 1.0, (4) 1.5, (5) 2.0, and (6) 2.5 mM. (B) Calibration curve consisting of the bioelectronic current plotted vs the acetone concentration. The error bars indicate the mean \pm standard deviation ($n = 3$).

turnover rate (TR_{max}) of 20 s⁻¹, using eq 3,⁴⁹

$$\text{TR}_{\text{max}} = \frac{I_{\text{cat}}^{\text{sat}} - I_0}{nFA\Gamma} \quad (3)$$

where I_0 is the background current, the y intercept of the calibration curve. The TR_{max} value represents the number of molecules of 2-propanol oxidized per 2° ADH molecule per second. To evaluate the reproducibility of the method, three bioelectronic interfaces were fabricated, and the current was measured for each at multiple 2-propanol concentrations. For 5, 15, and 25 mM, standard deviations were 8.9% ($n = 3$), 2.7% ($n = 3$), and 5.4% ($n = 3$), respectively. The standard deviation for the sensitivity was 6.0% ($n = 3$).

Figure 5A shows the amperometric response of the MPA-TBO-PEI-NADP⁺-2° ADH-modified electrode to 500 μM step increases in the acetone concentration in PBS, pH 7.4, under constant stirring at a constant potential of 400 mV. The resulting calibration curve, Figure 5B, shows that the steady-state anodic current increases linearly with concentration between 0.5 and 2.5 mM. The sensitivity and limit of detection were $5.6 \mu\text{A mM}^{-1}$ cm⁻² and 100 μM , respectively. The sensitivity and limit of detection were also determined to be $5.6 \mu\text{A mM}^{-1}$ cm⁻² and 100 μM , respectively, for 500 μM step increases in the 2-propanol concentration, measured at a potential of -200 mV. These results suggest that the MPA-TBO-PEI-NADP⁺-2° ADH-modified electrode can be used to measure the concentration of both 2-propanol and acetone. The 2° ADH-integrated electrodes exhibited 3% degradation in activity after continuous operation for 24 h at room temperature. When stored in a 0.1 M borate buffer (pH 7.5) solution at room temperature for 2 weeks, the electrodes exhibited no measurable loss in performance.

Table 1 shows the response of the MPA-TBO-PEI-NADP⁺-2° ADH-modified electrode to alternative substrates.

(49) Eisenwie, Hg; Schulz, G. V. *Naturwissenschaften* **1969**, *56* (11), 563-&.

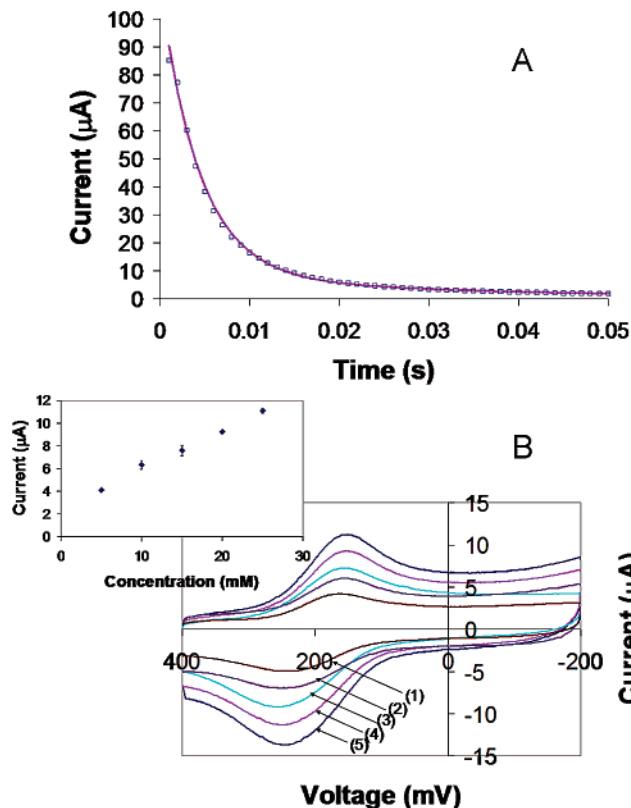


Figure 6. (A) Chronoamperometric current transient following a potential step from $E_{\text{initial}} = -200$ mV to $E_{\text{final}} = +400$ mV for the MPA-TBO-PEI-NADP⁺-2° ADH-functionalized electrode after reconstitution on the interface. (B) Cyclic voltammograms of the reconstituted MPA-TBO-PEI-NADP⁺-2° ADH functionalized electrode in the presence of different concentrations of 2-propanol: (1) 5, (2) 10, (3) 15, (4) 20, and (5) 25 mM. The data were recorded in room-temperature PBS at a potential scan rate of 100 mV s⁻¹. Inset: peak electrocatalytic current at various 2-propanol concentrations. The error bars indicate the mean \pm standard deviation ($n = 3$).

Table 1. Selectivity of the MPA-TBO-PEI-NADP⁺-2° ADH-Modified Electrode for the Substrates 2-Propanol, Ethanol, 2-Butanol, and 2-Pentanol

compd	$I_{\text{cat}}^{\text{sat}}$ (μA)	sensitivity ($\mu\text{A mM}^{-1} \text{cm}^{-2}$)
2-propanol	11.7 \pm 0.6	2.47 \pm 0.15
ethanol	4.7 \pm 0.4	0.49 \pm 0.04
2-butanol	4.5 \pm 0.6	0.37 \pm 0.05
2-pentanol	4.5 \pm 0.5	0.27 \pm 0.04

The sensitivities to 2-propanol, ethanol, 2-butanol, and 2-pentanol were 2.5, 0.49, 0.37, and 0.27 $\mu\text{A mM}^{-1} \text{cm}^{-2}$, respectively. The relative reaction rates for these substrates are consistent with literature values for *T. ethanolicus* 2° ADH, which indicates that 2° ADH activity decreases for alcohols larger than 2-propanol.^{50,51}

Figure 6A shows the chronoamperometric response of the bioelectronic interfaces following removal, and then reconstitution, of the NADP⁺-2° ADH-modified PEI layer to a potential step from -200 to +400 mV. Fitting eqs 1 and 2 to the chronoamperometric data gave k_{et} and Γ values of 230 s⁻¹ and 1.4×10^{-11} mol cm⁻², respectively. Figure 6B shows the cyclic voltammograms for oxidation of 2-propanol at the regenerated MPA-TBO-PEI-NADP⁺-2° ADH-modified electrode. The

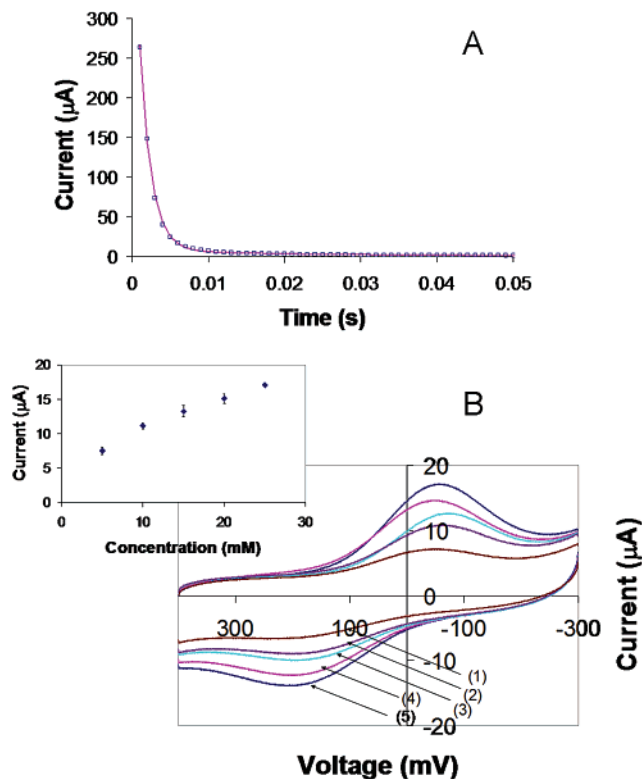


Figure 7. (A) Chronoamperometric current transient following a potential step from $E_{\text{initial}} = -200$ mV to $E_{\text{final}} = +400$ mV for the MPA-TBO-PEI-NADP⁺-SDH-functionalized electrode. (B) Cyclic voltammograms of MPA-TBO-PEI-NADP⁺-SDH in the presence of different concentrations of D-sorbitol: (1) 5, (2) 10, (3) 15, (4) 20, and (5) 25 mM. The data were recorded in room-temperature PBS at a potential scan rate of 100 mV s⁻¹. Inset: peak electrocatalytic current at various D-sorbitol concentrations. The error bars indicate the mean \pm standard deviation ($n = 3$).

Table 2. Selectivity of the MPA-TBO-PEI-NADP⁺-SDH-Modified Electrode for the Substrates D-Sorbitol, Xylitol, D-Mannitol, and D-Glucose

compd	$I_{\text{cat}}^{\text{sat}}$ (μA)	sensitivity ($\mu\text{A mM}^{-1} \text{cm}^{-2}$)
D-sorbitol	17.1 \pm 0.8	2.88 \pm 0.12
xylitol	4.1 \pm 0.4	0.24 \pm 0.02
D-mannitol	3.2 \pm 0.3	0.13 \pm 0.01
D-glucose	2.9 \pm 0.3	0.06 \pm 0.01

peak anodic current increased linearly with the 2-propanol concentration, with sensitivity and peak current density values of 2.1 $\mu\text{A mM}^{-1} \text{cm}^{-2}$ and 11 μA , respectively (Figure 6B, inset). The TR_{max} was calculated to be 19 s⁻¹ using eq 3. These values of k_{et} , Γ , $I_{\text{cat}}^{\text{sat}}$, TR_{max} for the regenerated MPA-TBO-PEI-NADP⁺-2° ADH-modified interface are similar to those for the original layer, indicating that the MPA-TBO-PEI-NADP⁺-2° ADH-modified interface is renewable.

To demonstrate the versatility of the approach, a bioelectronic interface was assembled using SDH instead of 2° ADH. SDH catalyzes the reversible oxidation of sorbitol to fructose using NAD⁺ as a cofactor. Figure 7A shows the chronoamperometric current for the MPA-TBO-PEI-NADP⁺-SDH-modified electrode in the presence of D-sorbitol following a potential step from -200 to +400 mV. While NADP⁺ has a single *cis*-diol group that can bind to the boronic acid, NAD⁺ has two, so two binding modes are feasible. For this reason, a biexponential decay model (eq 4) was used to analyze the data,¹⁴

$$I = k_{\text{et}}' Q' \exp(-k_{\text{et}}' t) + k_{\text{et}}'' Q'' \exp(-k_{\text{et}}'' t) \quad (4)$$

(50) Burdette, D.; Zeikus, J. G. *Biochem. J.* **1994**, *302*, 163–170.

(51) Burdette, D. S.; Secundo, F.; Phillips, R. S.; Dong, J.; Scott, R. A.; Zeikus, J. G. *Biochem. J.* **1997**, *326*, 717–724.

where k_{et}' and k_{et}'' are the electron-transfer rate constants for the two binding modes and Q' and Q'' are the corresponding amounts of charge transferred by each binding mode. The resulting k_{et}' and k_{et}'' values were 650 and 53 s^{-1} and the corresponding Γ values were determined to be 1.5×10^{-11} and 4.5×10^{-12} mol cm^{-2} , respectively, using eq 2.

Figure 7B shows cyclic voltammograms for the oxidation of D-sorbitol at the MPA-TBO-PEI-NAD⁺-SDH-modified electrode. The peak current increased linearly with the D-sorbitol concentration (Figure 7B, inset), with a sensitivity of 2.9 $\mu\text{A mM}^{-1} \text{cm}^{-2}$. At higher concentrations, the anodic current reached a saturation value of 17 μA . The TR_{max} was calculated using eq 3 to be 18 s^{-1} . To evaluate the reproducibility of the biosensor fabrication method, three bioelectronic interfaces were fabricated, and the currents for these different interfaces were measured at D-sorbitol concentrations of 5, 15, and 25 mM. The standard deviations were 7.1% ($n = 3$), 6.2% ($n = 3$), and 0.5% ($n = 3$), respectively. The standard deviation for the sensitivity was 4.1% ($n = 3$).

At a constant potential of 400 mV, the MPA-TBO-PEI-NAD⁺-SDH-modified electrode gave a steady-state anodic current that increased linearly with the D-sorbitol concentration between 1 and 5 mM (data not shown). The sensitivity and limit of detection were 1.0 $\mu\text{A mM}^{-1} \text{cm}^{-2}$ and 100 μM , respectively. The SDH-integrated electrodes exhibited 3% degradation in activity after continuous operation for 24 h at room temperature. Upon storage in room-temperature borate buffer (pH 7.0), and daily calibration, the bioelectronic interface's sensitivity decreased to 50% of its original value after 14 days.

Table 2 shows the response of the MPA-TBO-PEI-NAD⁺-SDH-modified electrode to alternative substrates. The sensitivities to D-sorbitol, xylitol, D-mannitol, and D-glucose were 2.9, 0.24, 0.13, and 0.06 $\mu\text{A mM}^{-1} \text{cm}^{-2}$, respectively. The relative reaction rates for these substrates are consistent with literature values for SDH from *Pseudomonas* sp. specificity.⁴⁰

The novel approach presented here uses functionalized polyelectrolytes to fabricate bioelectronic interfaces that can be removed by a simple pH change and then reconstituted. For the enzymes tested, 2° ADH and SDH, the $I_{\text{cat}}^{\text{sat}}$, sensitivity, and TR_{max} values of the reconstituted interface were comparable to those of the original. The ability to reconstitute bioelectronic interfaces without affecting their performance can greatly reduce

the operating costs of bioelectronic processes by allowing the electrode materials to be reused and the bioelectronic interface to be regenerated quickly and inexpensively. Our novel interface has potential applications for biosensors, bioreactors, and biofuel cells. Moreover, because the method is based on LbL self-assembly, it is compatible with microfluidic processes and assembly on high-density biosensor arrays.

Conclusions

A novel bioelectronic interface for dehydrogenase enzymes has been developed, in which an electron mediator was first covalently bound to a negatively charged gold electrode, and then positively charged polyelectrolytes functionalized with the enzyme and its cofactor were bound by electrostatic interactions. Cyclic voltammetry, chronoamperometry, constant potential amperometry, electrochemical impedance spectroscopy, and Fourier transform infrared spectroscopy analyses were used to demonstrate sequential assembly of the layers and to characterize the performance properties of the resulting bioelectronic interfaces. The labile components of the interface, the cofactor and enzyme, were able to be removed by a decrease in pH and then reconstituted to regenerate the bioelectronic interface. The saturation current, sensitivity, and turnover rate for the MPA-TBO-PEI-NADP⁺-2° ADH-modified interface before the removal were 12 μA , 2.5 $\mu\text{A mM}^{-1} \text{cm}^{-2}$, and 20 s^{-1} , respectively, compared to 11 μA , 2.1 $\mu\text{A mM}^{-1} \text{cm}^{-2}$, and 19 s^{-1} , respectively, for the reconstituted bioelectronic interface. The versatility of the approach was demonstrated through the use of two dehydrogenase enzymes (2° ADH and SDH) and two cofactors (NADP⁺ and NAD⁺). The ability to renew bioelectronic interfaces is a novel capability that has potential applications for biosensors, biocatalytic reactors, and biological fuel cells.

Acknowledgment. We thank the Kikkoman Corp. (Chiba, Japan) for donating purified SDH. This work was funded by grants from the Department of Education GAANN Program, National Science Foundation (CTS-0609164), Michigan Economic Development Corp. through its Michigan Technology Tri-Corridor program, and MSU Intramural Research Grants Program and an MSU Strategic Partnership Grant.